Processing of information from the parafascicular nucleus of the thalamus through the basal ganglia

Maroua Hanini-Daoud, Florence Jaouen, Pascal Salin, Lydia Kerkerian-Le Goff, Nicolas Maurice

Received: 13 August 2021 | Revised: 8 March 2022 | Accepted: 15 March 2022

DOI: 10.1002/jnr.25046

RESEARCH ARTICLE

JOURNAL OF Neuroscience Research

Processing of information from the parafascicular nucleus of the thalamus through the basal ganglia

Maroua Hanini-Daoud | Florence Jaouen | Pascal Salin | Lydia Kerkerian-Le Goff | Nicolas Maurice

Aix Marseille Univ, CNRS, IBDM, Marseille, France

Correspondence
Nicolas Maurice, Aix Marseille Univ, Institut de Biologie du Développement de Marseille (IBDM), CNRS UMR 7288, Case 907, Parc Scientifique de Luminy, 13288 Marseille Cedex 9, France.
Email: nicolas.maurice@univ-amu.fr

Present address
Nicolas Maurice, Aix Marseille Univ, Institut de Neurosciences de la Timone (INT), CNRS UMR 7289, Campus Santé Timone, 27 Boulevard Jean Moulin, Marseille Cedex 05, 13885, France

Funding information
Fondation de France

Abstract

Accumulating evidence implicates the *parafascicular nucleus* of the thalamus (Pf) in basal ganglia (BG)-related functions and pathologies. Despite Pf connectivity with all BG components, most attention is focused on the thalamostriatal system and an integrated view of thalamic information processing in this network is still lacking. Here, we addressed this question by recording the responses elicited by Pf activation in single neurons of the *substantia nigra pars reticulata* (SNr), the main BG output structure in rodents, in anesthetized mice. We performed optogenetic activation of Pf neurons innervating the striatum, the subthalamic nucleus (STN), or the SNr using virally mediated transcellular delivery of Cre from injection in either target in Rosa26-LoxP-stop-ChR2-EYFP mice to drive channelrhodopsin expression. Photoactivation of Pf neurons connecting the striatum evoked an inhibition often followed by an excitation, likely resulting from the activation of the trans-striatal direct and indirect pathways, respectively. Photoactivation of Pf neurons connecting the SNr or the STN triggered one or two early excitations, suggesting partial functional overlap of trans-subthalamic and direct thalamonigral projections. Excitations were followed in about half of the cases by an inhibition that might reflect recruitment of intranigral inhibitory loops. Finally, global Pf stimulation, electrical or optogenetic, elicited similar complex responses comprising up to four components: one or two short-latency excitations, an inhibition, and a late excitation. These data provide evidence for functional connections between the Pf and different BG components and for convergence of the information processed through these pathways in single SNr neurons, stressing their importance in regulating BG outflow.

KEYWORDS
basal ganglia, *in vivo* electrophysiology, intralaminar nuclei of the thalamus, optogenetics, RRID:AB_10000240, RRID:AB_162543, RRID:AB_2209751, RRID:AB_2301751, RRID:AB_2337244, RRID:AB_2340375, RRID:AB_2535718, RRID:IMSR_EM:01153, RRID:IMSR_JAX:012569, *substantia nigra pars reticulata*

1 | INTRODUCTION

The parafascicular nucleus of the thalamus (Pf) is the primary subcortical source of excitatory afferents to the basal ganglia (BG), where it mainly targets the striatum, the major input station of the network. Over the last 20 years, significant knowledge has been gained on the complex anatomy, physiology, and functions of the microcircuits linking the Pf with the cerebral cortex and the

Edited by Cristina Antonella Ghiani and Joshua L. Plotkin. Reviewed by Yoland Smith, Xiaohui Lv and Qiaoling Cui

striatum (Mandelbaum et al., 2019; Smith et al., 2009), in particular its robust link with the striatal cholinergic interneurons (Lapper & Bolam, 1992; Sidibé & Smith, 1999) that are now viewed as central regulators of striatal functions (Abudukeyoumu et al., 2019). Hence, major progress has been made in the dissection of the network mechanisms underlying the proposed key role of the Pf projections to the striatum in processes as redirection of attention, associative learning, correct action selection in an ongoing sensorimotor context, and behavioral flexibility (Brown et al., 2010; Ding et al., 2010; Mandelbaum et al., 2019; Matsumoto et al., 2001; Yamanaka et al., 2018). Renewed interest for the Pf, long neglected in the models of BG functioning, also arose from clinical and experimental data supporting its involvement in the pathophysiology of BG-related disorders, including Parkinson's disease and Tourette's syndrome, and the potential of its deep brain stimulation to alleviate symptoms of these diseases (Fasano et al., 2012; Henderson et al., 2000; Ilyas et al., 2019; Kerkerian-Le Goff et al., 2009; Lanciego et al., 2009; Smith et al., 2004; Stefani et al., 2009; Testini et al., 2016; Watson et al., 2021).

Among the thalamic nuclei, the Pf is characterized by its widespread connectivity with the entire BG network, contrasting with its relatively sparse, although highly organized, connections with the cerebral cortex. Besides its heavy input to the striatum, it provides weak to moderately dense inputs to all the BG components (Bevan et al., 1995; Castle et al., 2005; Deschênes et al., 1996; Lanciego et al., 2004; Marini et al., 1999; Sadikot et al., 1992; Tandé et al., 2006; Yasukawa et al., 2004) and, in turn, receives a substantial innervation from the BG output structures (Sadikot & Rymar, 2009). Single axon reconstruction showed that some Pf axons give rise to collaterals that arborize within the striatum and extrastriatal BG components (Deschênes et al., 1996), including the subthalamic nucleus (STN) that is also considered as an input station of the BG. However, dual retrograde tracing study provided evidence that projections to the striatum and to the STN mostly arise from distinct neuronal populations of the Pf (Féger et al., 1994), which has been recently confirmed using a combination of Cre-dependent retrograde viruses (Watson et al., 2021). Whether or not Pf neurons projecting to different extrastriatal targets are also mostly segregated has not been investigated in depth. Furthermore, contrasting with the increasing knowledge on the function of the projections of this thalamic complex to the striatum, little is known about the functional contributions of the subcircuits it forms with the other BG components. The importance of these issues is pointed out by a recent study demonstrating that the projections to STN while not to striatum contribute to movement initiation (Watson et al., 2021).

The present study was undertaken to provide an integrated view of thalamic information processing through the BG network. To do so, we combined *in vivo* electrophysiological recordings of neurons in the *substantia nigra pars reticulata* (SNr), the main basal ganglia output structure in rodents, with stimulation of Pf, either electrical or by optogenetics, in anesthetized mice. We recorded the responses evoked by stimulating neuronal Pf subpopulations distinguished on the basis of their connectivity with the striatum, the STN or the SNr, respectively, and of Pf neurons taken as a whole, to decipher the contribution of the different circuits to the global responses. The results show that trans-striatal, trans-subthalamic, and direct thalamonigral circuits are functional and can convey converging information onto single SNr neurons. They provide evidence for segregation of the information transferred through the striatum and through extrastriatal pathways, but for partial functional overlap between the trans-subthalamic and thalamonigral pathways, as also confirmed by retrograde tracing experiments. Finally, they highlight the Pf-evoked responses recorded in the SNr as a readout of the functionality of the different pathways by which the Pf impacts BG outflow.

Significance

The thalamic centromedian/parafascicular (CM/Pf) complex is a major input and output station of the basal ganglia (BG). While increasing knowledge is gained on the thalamostriatal circuitry, the functional connectivity of the parafascicular nucleus (Pf) with the other BG components and the integration of the information it provides to the network are poorly understood. By combining *in vivo* electrophysiological recordings with electrical or optogenetic stimulation, we show that neuronal activity in the BG output structure can be shaped by convergent information processed through trans-striatal, trans-subthalamic, and direct thalamonigral subcircuits. Such high level of integration suggests an important functional weight of these different pathways on BG outflow, which needs to be considered to fully appreciate Pf implication in BG physiological and pathological functioning.

2 | MATERIALS AND METHODS

Animal experimental procedures were approved by the Comité National de Réflexion Ethique sur l'Expérimentation Animale (Comité d'éthique de Marseille # 14) and were in agreement with the European Communities Council Directive (2010/63/EU). All surgical procedures and electrophysiological recordings were conducted in mice anesthetized with intraperitoneal (i.p.) injections of ketamine and xylazine (100 and 10 mg/kg, respectively).

2.1 | Mice

We used CamKIIα-IRES-Cre BAC mice (CamKII$^{cre/+}$ mice, purchased through European Mouse Mutant Archive, ID:EM01153, RRID:IMSR_EM:01153) and Rosa26-LoxP-stop-ChR2-EYFP mice (ChR2-EYFP mice, purchased from Jackson Laboratories, stock

number: 012569, RRID:IMSR_JAX:012569). Both strains were maintained on C57Bl/6J genetic background and both sexes were used for ethical considerations.

2.2 | Virally mediated expression of opsins in Pf neurons

To drive channelrhodopsin (ChR2) expression in Pf neurons, we used two different AAV vectors containing transgene to express either ChR2 (AAV-Ef1α-DIO-hChR2[H134R]-mCherry; titer: ≥10^{13} vg/ml) or Cre recombinase (AAV-EF1α-mCherry-IRES-WGA-Cre; titer: 1.6×10^{12} vg/ml). These recombinant AAV vectors were serotyped with AAV5 coat proteins and packaged by the viral vector core at the University of North Carolina (UNC Vector Core, Chapel Hill, NC).

Anesthetized mice were mounted on a stereotaxic apparatus (David Kopf Instruments, Tujunga, CA). Injections were made with a 10-µl syringe, connected to the injector (30 G) by a polyethylene tubing, and controlled by an injection pump at 0.3 µl/min.

To achieve Cre-dependent expression of ChR2 in Pf neurons independently on their projection site, we microinjected 1 µl of AAV-Ef1a-DIO-hChR2(H134R)-mCherry into the Pf of CamKII$^{cre/+}$ mice (−2.3 mm AP, ±0.7 mm ML, −3.1 mm DV). To achieve Cre-dependent expression of ChR2 in subpopulations of Pf neurons based on their connectivity with distinct BG nuclei, we applied a strategy relying on the transcellular transport of Cre using a virus expressing Cre recombinase fused to the tracer protein wheat germ agglutinin (AAV5-EF1α-mCherry-IRES-WGA-Cre; Gradinaru et al., 2010). Microinjections of this virus were performed in Rosa26-LoxP-stop-ChR2-EYFP mice into the striatum (1 µl at two dorso-ventral sites: +1.0 mm AP, +1.7 mm ML, −3.1 and −2.7 mm DV), the STN (0.2 µl at one site at: −1.8 mm AP, +1.6 mm ML, −4.5 mm DV), or the SNr (0.3 µl at one site: −2.8 mm AP, +1.35 mm ML, −4.4 mm DV), at coordinates defined from bregma with the incisor bar at −1.0 mm according to the stereotaxic mouse atlas of Paxinos and Franklin (2001). At the injection site, transduced cells can be visualized by mCherry immunodetection. These transduced cells express the Cre recombinase fused to the transcellular tracer WGA which is secreted locally, taken up by the axon terminals of synaptically connected neurons and transported to their cell body, which allows opsin expression only in the cells defined by this connectivity. ChR2-expressing neurons were visualized by immunodetection of either mCherry in CamKII$^{cre/+}$ mice or of EYFP in Rosa26-LoxP-stop-ChR2-EYFP. Cortical afferent terminals were visualized in the Pf by VGLUT1 immunolabeling. For primary antibody exposure, brain sections were incubated overnight at 4°C in Rabbit anti-RFP (#600-401-379, RRID:AB_2209751, Rockland), Chicken anti-GFP (#GFP-1020, RRID:AB_10000240, Aves Labs, Davis, CA), and/or Guinea Pig anti-VGLUT1 (#AB5905, RRID:AB_2301751, Merck) diluted to 1/1,000. Secondary antibodies were Alexa Fluor 555 Donkey anti-Rabbit (#A-31572, RRID:AB_162543, Invitrogen), Alexa Fluor 488 Donkey anti-Chicken (#703-545-155, RRID:AB_2340375, Jackson Immunotech, Cambridgeshire, UK), and/or Alexa Fluor 633 Goat anti-Guinea Pig (#A-21050, RRID:AB_2535718, Invitrogen) used at 1/500 for 1 hr 30 min at room temperature. See Table 1 for more details.

2.3 | Electrophysiological recordings

Mice under anesthesia were fixed in a stereotaxic frame (Horsley-Clarke apparatus, Unimécanique, Epinay-sur-Seine, France) and body temperature was maintained at 36.5°C. All recordings were performed 8–10 weeks after injection of the viruses. Single-unit activity of neurons in the SNr (at: −3.3/−2.9 mm AP, +1.3/+1.5 mm ML, −3.7/−4.6 mm DV) was recorded extracellularly using glass micropipettes (25–35 MΩ) filled with a 0.5M sodium chloride solution containing 1.5% neurobiotin (Vector Laboratories, Burlingame, CA). Action potentials were recorded using a Axoclamp-2B amplifier (Molecular Devices, Union City, CA), amplified, filtered with an AC/DC amplifier (DAM 50, Tektronix, Courtabœuf, France). Data were sampled online at 10 kHz rate on a computer connected to a CED 1401 interface and offline analyzed using Spike2 software (Cambridge Electronic Design, Cambridge, UK). Nigral neurons were identified as non-dopaminergic by their classically defined electrophysiological characteristics: narrow spikes (width ≤ 2 ms) and ability to present high-frequency discharge (>10 Hz) without decrease in spike amplitude (Bunney et al., 1973; Deniau et al., 1978).

2.4 | Pf stimulation and analysis of evoked responses

The Pf (at: −2.3 mm AP, +0.7 mm ML, −3.2 mm DV) ipsilateral to the recorded SNr was stimulated through either bipolar coaxial stainless steel electrode (SNE-100, Rhodes Medical Instruments, Woodlands Hill, CA) or optical fiber (NA 0.22, 200 µm diameter, Thorlabs, Canada). Electrical stimulation consisted of pulses of 600 µs width and 10–20 V, delivered at 1 Hz. Optical stimulation consisted of pulses of blue light (1 ms, Laser 473 nm, 180–200 mW) delivered at 1 Hz. Peristimulus time histograms (PSTHs) were generated from 140 stimulation trials with a bin size of 1 ms. Spikes were discriminated from noise and stimulation artifact based on their amplitude, using the gate function of a 121 window discriminator (World Precision Instruments) and sampled online. Excitatory responses were defined as >50% increase versus pre-stimulus in the number of spikes for at least three consecutive bins and were characterized by their latency, duration, and amplitude (number of spikes within the excitatory response period minus the mean number of spontaneous spikes emitted in basal condition within the same duration of time). Inhibitory responses corresponded to the time interval during which no spike was observed and were characterized by their latency and duration. Given the maintenance of a sustained tonic activity of SNr neurons despite the decrease in their firing rate in our anesthetized animals, inhibitory responses can be evidenced from 60 stimulations as previously documented following cortical stimulations (Maurice et al., 1999). Only responses obtained from animals with both a

TABLE 1 Antibody table

Antibody name	Immunogen	Catalog number/RRID	Clonality	Host organism	Concentration
RFP antibody pre-adsorbed	Red fluorescent protein (RFP) fusion protein corresponding to the full-length amino acid sequence (234aa) derived from the mushroom polyp coral discosoma	Rockland Cat# 600-401-379, RRID:AB_2209751	Polyclonal antibody	Rabbit	1/1,000
Green fluorescent protein (GFP) antibody	Purified recombinant green fluorescent protein (GFP) emulsified in Freund's adjuvant	Aves Labs Cat# GFP-1020, RRID:AB_10000240	Polyclonal antibody	Chicken	1/1,000
Guinea pig anti-vesicular glutamate transporter 1 (VGLUT1) polyclonal antibody, unconjugated	Synthetic peptide from rat VGLUT1 protein with no overlap to VGLUT2. The immunogen is available as AG208	Millipore Cat# AB5905, RRID:AB_2301751	Polyclonal antibody	Guinea pig	1/1,000
Donkey anti-rabbit IgG (H+L) highly cross-adsorbed secondary antibody, Alexa Fluor 555	Rabbit gamma immunoglobins heavy and light chains	Molecular Probes Cat# A-31572, RRID:AB_162543	Polyclonal antibody	Donkey	1/500
Alexa Fluor 488 AffiniPure Donkey anti-chicken IgY (IgG) (H+L) antibody	IgY (IgG) (H+L) chicken	Jackson ImmunoResearch Labs Cat# 703-545-155, RRID:AB_2340375	Polyclonal antibody	Donkey	1/500
Goat anti-mouse IgG (H+L) cross-adsorbed secondary antibody, Alexa Fluor 633	IgG (H+L) mouse	Thermo Fisher Scientific Cat# A-21050, RRID:AB_2535718	Polyclonal antibody	Goat	1/500
Cy3-streptavidin		Jackson ImmunsoResearch Labs Cat# 016-160-084, RRID:AB_2337244			1/1,000

correct targeting of injection sites and a correct positioning of the optical fiber and the recording electrodes were analyzed. Numerical values are given as means ± *SEM*. Statistical analysis was performed using Prism 9 (GrapPad Software, San Diego, CA). Statistically significant differences were tested using Student's *t*-test or Mann–Whitney Rank Sum test as indicated for each situation. Significance level was set at $p < 0.05$. Numerical *p*-values and corresponding *n*-values are given in Table 2.

2.5 | Juxtacellular labeling using neurobiotin

Some Pf neurons were juxtacellularly labeled with neurobiotin according to Pinault (1996). Briefly, positive current pulses (2–6 nA, 200 ms, 50% duty cycle) were applied until single-unit activity became robustly entrained by the pulses for at last 5 min. Two to four hours after labeling, mice were euthanized by a lethal dose of anesthetic and transcardially perfused with 5 ml sodium chloride solution followed by 20 ml of 4% paraformaldehyde in phosphate buffer (PBS). Brains were removed and cryoprotected in sucrose 30% in PB and frozen until cutting. Serial frozen section (40 µm) were incubated overnight at room temperature in Triton (0.3%) phosphate buffer saline (PBS) containing Cy3-streptavidin (1:1,000, RRID:AB_2535718, Thermo Fisher Scientific).

2.6 | Retrograde labeling with cholera toxin subunit B (CTB)

Three adult (8–10 weeks) mice under anesthesia were placed in a David Kopf stereotaxic apparatus. Small craniotomies were made on the skull. Solutions of 150 nl of cholera toxin subunit B (CTB) conjugated to Alexa Fluor 594 (#C34777, Molecular probes, Eugene, OR) and Alexa Fluor 488 (#C34775, Molecular probes) at 1 µg/µl in PBS were pressure-injected through a Hamilton syringe at a flow rate of 30 nl/min in the SNr and in the STN, respectively. The stereotaxic coordinates of the injection sites were as follows: SNr: −2.7 mm AP, +1.3 mm ML, −4.4 mm DV; STN: −1.7 mm AP; +1.6 mm ML; −4.35 mm DV. A similar experiment was performed consisting of injections of CTB conjugated to Alexa Fluor 488 (150 nl) in the STN combined with injections of CTB conjugated Alexa Fluor 594 (450 nl) in the striatum (+1.0 mm AP, +1.7 mm ML, −2.9 mm DV) in three additional mice. After surgery, mice were injected with 5 mg/kg carprofen (Rimadyl®, Pfizer) to reduce postoperative inflammation

TABLE 2 Characteristics of the responses evoked in SNr cells by electrical or optical stimulation of the Pf

	Early excitation			2nd excitation			Inhibition		Late excitation		
	L (ms) (N)	D (ms) (N)	Nb Sp (N)	L (ms) (N)	D (ms) (N)	Nb Sp (N)	L (ms) (N)	D (ms) (N)	L (ms) (N)	D (ms) (N)	Nb Sp (N)
Electrical stim. (54)	4.4 ± 0.4 (27)	6.1 ± 0.7 (27)	40.0 ± 6.2 (27)	10.6 ± 0.6 (26)	6.6 ± 0.6 (26)	39.9 ± 5.0 (26)	14.8 ± 1.0 (37)	18.4 ± 2.2 (37)	29.4 ± 2.6 (22)	20.3 ± 4.5 (22)	62.1 ± 17.2 (22)
Optical stim. (41)	4.3 ± 0.3 (19) ns	7.2 ± 0.7 (19) ns	60.7 ± 10.6 (19) ns	8.4 ± 0.9 (11)*	6.6 ± 0.7 (11) ns	52.4 ± 11.4 (11) ns	20.1 ± 1.0 (36)*	20.5 ± 1.4 (36) ns	42.7 ± 3.1 (8)*	18.5 ± 2.8 (8) ns	39.0 ± 8.3 (8) ns
	$U = 241.5$	$U = 191.5$	$U = 198$	$U = 74$	$U = 134.5$	$U = 112$	$U = 349.5$	$U = 492$	$U = 34$	$U = 74$	$U = 88$
	$p = 0.7385$	$p = 0.1467$	$p = 0.1957$	$p = 0.0184$	$p = 0.7833$	$p = 0.3125$	$p = 0.0004$	$p = 0.0547$	$p = 0.0095$	$p = 0.5261$	$p > 0.9999$

Note: Statistical comparisons of the parameters of the responses evoked by electrical stimulation versus optical stimulation were performed using Mann–Whitney rank sum test: *, significantly different; ns, no significant; Stim., stimulation.

and pain. Ten days after CTB injection, mice were anesthetized and perfused intracardially with 5 ml NaCl (0.9%) followed by 30 ml paraformaldehyde (4% in 0.12M PBS pH 7.2). Dissected brains were post-fixed in paraformaldehyde (4% in PBS) overnight at 4°C and kept in a cryoprotective solution containing 30% of sucrose at 4 °C for 2 days and then frozen in dry ice and stored at −80°C. Frozen coronal (40 μm thick) tissue sections were cut at −20°C with a cryostat (CM3050, Leica, Nussloch, Germany) at Pf level. The sections were then mounted on SuperFrost Plus glass slides (Fisher Scientific, Elancourt, France). The sections were inspected under a Zeiss confocal microscope (510 Meta, Zeiss, Oberkochen, Germany) at low magnification. Colocalization analysis into the Pf was performed by counting the number of cells labeled both with CTB conjugated to Alexa Fluor 594 and CTB conjugated to Alexa Fluor 488 in 13 coronal sections for the combined injections in the SNr and STN or in nine coronal sections for the combined injections in the STN and the striatum. Photomicrographs were obtained at the highest magnification available (63× oil-immersion lens, NA 1.4; 1,024 × 1,024 pixels) and with the appropriate band-pass and long-pass filter setting to avoid cross-talk.

3 | RESULTS

3.1 | SNr responses elicited by optogenetic activation of subpopulations of pf neurons distinguished on the basis of their connectivity

The Pf is connected to the SNr through different BG pathways, including the trans-striatal, trans-subthalamic, and the direct thalamonigral pathways. To assess the functionality of these different pathways, we recorded the responses elicited in SNr neurons by the optogenetic activation of subpopulations of Pf neurons segregated based on their connections with the striatum, STN, or SNr, respectively (Figure 1). This connectivity-based strategy relies on the expression of the opsin in the projection neurons innervating a given target owing to the transcellular transport of Cre from this target, using virally mediated expression of the WGA-Cre. For instance, 5 weeks after the unilateral injection of the virus into the striatum of Rosa26-LoxP-stop-ChR2-EYFP mice, robust ChR2-EYFP expression was observed in a large subset of Pf neurons strictly in the ipsilateral side (Figure 2a), in few other thalamic nuclei, notably the ventral posteromedial (VPM) nucleus, as well as in other neuronal populations known as innervating the striatum, such as cortical projection neurons and nigral dopaminergic cells (data not shown). Although the opsin was expressed in all the systems innervating the virally injected structure, restricted activation of the Pf thalamic projection system was achieved by light delivery into the Pf. The limitation of this strategy might be the recruitment, besides Pf neurons projecting to either targets, of axon collaterals within the Pf of other neuronal systems projecting to the injected BG component. Previous work in the cat using dual retrograde tracing provided evidence for collateralized projections from the cerebral cortex to the Pf and the striatum (Paré & Smith, 1996; Royce, 1983), although the number of double

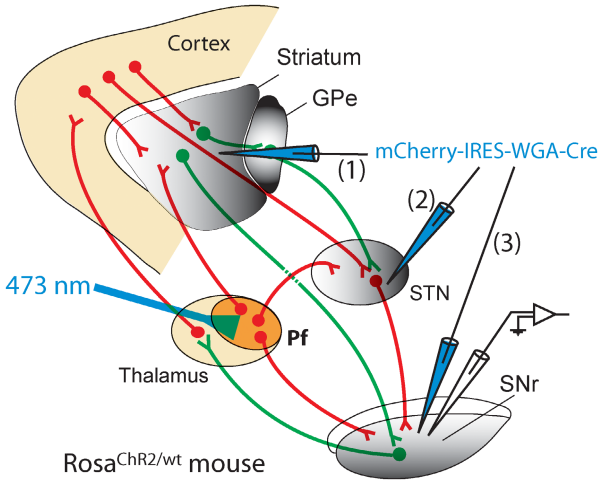

FIGURE 1 Schematic of the strategy used to assess the functionality of the thalamostriatal, thalamosubthalamic, and thalamonigral pathways. In three different sets of experiments, expression of WGA-Cre was achieved by viral delivery of mCherry-IRES-WGA-Cre into the striatum (1), the subthalamic nucleus (STN; 2), or the *substantia nigra pars reticulata* (SNr, 3) in Rosa26-LoxP-stop-ChR2-EYFP mice. ChR2 is expressed in the locally transduced neurons, and, after transneuronal retrograde transport of WGA-Cre, in the connecting ones, including the Pf projection neurons. Light was then delivered in the Pf to activate the neuronal subpopulation connecting the virally injected basal ganglia target, and the evoked responses were recorded in the SNr. GPe, external segment of the *globus pallidus*; Pf, *parafascicular nucleus* of the thalamus; SNr, *substantia nigra pars reticulata*; STN, *subthalamic nucleus*

labeled cortical neurons was few compared to the single labeled ones from either target (Royce, 1983). To investigate the potential implication of Pf collaterals of corticostriatal projections which could result in axonal reflex in our experimental paradigm, we labeled cortical terminals into the Pf using VGLUT1 immunoreactivity as a specific marker in Rosa26-LoxP-stop-ChR2-EYFP mice after WGA-Cre viral injection into the striatum (Figure 2b). VGLUT1 and EYFP immunostained profiles were spatially segregated, suggesting that cortico-Pf fibers are not expressing ChR2 at detectable level following WGA-Cre viral delivery into the striatum and thus will not be recruited by Pf light shining. The next step was to validate the functionality of the ChR2 by performing single-unit extracellular recordings of Pf neurons. As illustrated in Figure 2c, some of the recorded Pf neurons were efficiently driven by 1 ms blue light pulses, and their juxtacellular labeling with neurobiotin showed that these light-driven neurons actually expressed ChR2-EYFP, confirming the efficiency of our optogenetic strategy.

The impact of the specific activation of the Pf-striatal circuit was then investigated in SNr neurons (Figure 3). Figure 3a illustrates the WGA-Cre expression in the virally injected striatum and the expression of ChR2 in the synaptically connected Pf neurons in a mice used for electrophysiological recordings. A large number of both transduced cells in the striatum (Figure 3a1) and of ChR2-expressing cells in the PF (Figure 3a2), as reported in Figure 2a1, was consistently observed in the recorded animals. Photo-activation of the Pf neurons projecting to the striatum evoked responses in 22 out of 68 recorded SNr cells. Among the responding cells, 10 presented an inhibition followed by an excitation (Figure 3b), 8 cells displayed only an inhibition (Figure 3c), whereas the 4 remaining neurons showed only late excitation (not shown). The population PSTH in Figure 3d depicts two components in the average response, namely an inhibition followed by an excitation, whose characteristics are detailed in Figure 3e. It is to note that there was a competition between the inhibition and the following excitation. This was evidenced by the fact that (i) the inhibition was longer (21.5 ± 2.0 ms vs. 14.1 ± 2.1 ms; $t[16] = 2.525$; $p = 0.023$; Student's *t*-test) when it was not followed by an excitation ($n = 8$) and (ii) the excitation, when alone ($n = 4$), had a shorter latency (18.1 ± 5.0 ms vs. 35.2 ± 4.2 ms; $t[12] = 2.334$; $p = 0.038$; Student's *t*-test), a tendency for a longer duration (23.0 ± 4.8 ms vs. 14.3 ± 1.7 ms; $t[12] = 2.155$; n.s. $p = 0.052$; Student's *t*-test) and a stronger amplitude (71.1 ± 21.7 spikes vs. 19.7 ± 4.4 spikes; $U = 3$; $p = 0.014$: Mann–Whitney rank sum test).

Next, the impact of the specific activation of the Pf-subthalamic circuit was examined. Figure 4a illustrates an injection site in the STN (Figure 4a1) and the transcellularly driven expression of ChR2 in the connected Pf neurons (Figure 4a2). Photo-activation of Pf neurons projecting to the STN evoked responses in 8 out of 78 examined SNr cells. These responses consisted of one (6/8) or two early excitations (2/8), followed, in most of the cases ($n = 5$, 62.5%), by an inhibition, as illustrated in Figure 4b. The population PSTH (Figure 4c) further shows that the excitations are distributed in two peaks with latencies <5 ms or ≥5 ms. Characteristics of the population responses are detailed in Figure 4d.

Finally, the impact of the specific activation of the direct thalamonigral projection system was assessed. Figure 5a depicts an injection site in the SNr (Figure 5a1) and the retrogradely driven expression of ChR2 in the connected Pf neurons (Figure 5a2). Out of the virally injected BG components, SNr is the one from which the weaker ChR2 expression is found in the Pf. Photo-activation of Pf neurons projecting to SNr evoked responses in 14 out of 53 recorded SNr cells. These responses consisted of a single (12/14, Figure 5c) or a double excitation (2/14, Figure 5b) followed, in half of the cells, by an inhibition. Population PSTH in Figure 5d evidences these excitations followed by the inhibition in the average population response. The distribution displays a peak with a shoulder reminiscent of the second peak of the trans-STN responses (≥5 ms, see also Figure 4c). We then used the same latency thresholds (<5 ms or ≥5 ms) to distinguish the two excitations and provide the characteristics of the population responses (Figure 5e).

3.2 | SNr responses evoked by stimulating Pf neuronal populations as a whole

We then investigated the global transfer of information from the Pf through the BG, by recording the responses elicited in SNr neurons by Pf stimulation, either electrically or by optogenetics.

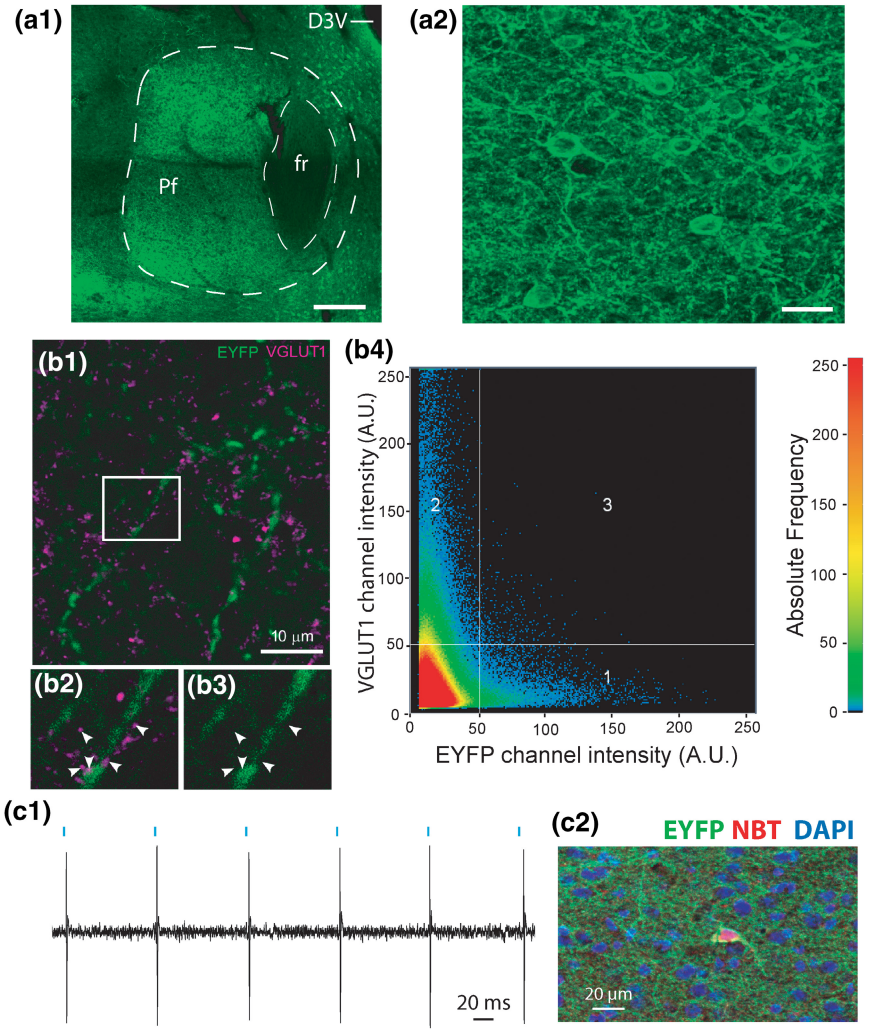

FIGURE 2 Optogenetic strategy to activate subpopulations of Pf neurons distinguished on the basis of their connectivity with BG components: Example of the thalamostriatal neurons. (a) Channelrhodopsin expression in the Pf as revealed by EYFP immunodetection in coronal brain slices following injection of AAV carrying the EF1α::mCherry-IRES-WGA-Cre cassette in the striatum (maximum intensity projection, 40 µm depth). A strong labeling was observed in the ipsilateral Pf (a1 and a2 at higher magnification) but not in the contralateral side. (b1) relationship between EYFP expressing neurites and VGLUT1 expressing axon terminals (single confocal section). (b2,b3) Higher magnification of the boxed area in b1 showing the absence of EYFP immunolabeling in VGLUT1 axon terminals. (b4) colocalization analysis of EYFP and VGLUT1 fluorescence confirms that the two markers are spatially segregated. (c) efficiency of the optogenetic strategy. Raw trace recording of a pf neuron (c1) whose firing was driven by 1 ms-blue light pulses (10 Hz). The cell body of this recorded neuron juxtacellularly labeled with neurobiotin (NBT, red) also shows EYFP immunolabeling (green) indicating that it actually expressed ChR2 (c2). A.U., arbitrary unit; DAPI, 4′,6-diamidino-2-phenylindole; *EYFP*, *enhanced yellow fluorescent protein*; Fr, *fasciculus retroflexus*; *NBT*, *Neurobiotin*; Pf, *parafascicular nucleus of the thalamus*; *VGLUT1*, Vesicular glutamate transporter 1. Scale bars: 200 µm in a1 and 20 µm in a2

Responses evoked by electrical stimulation of the Pf were analyzed in 54 SNr responding cells recorded in 18 mice (Figure 6). They presented up to four components: one or two early excitations, an inhibition, and a late excitation. Inhibition was recorded in the majority of the cells (n = 37 of 54; 68.5%), the most often (30 of 37), preceded by one or two short latency excitations (Figure 6a–c). The inhibition was in some cases followed by a late excitation (13 out of 37 cells) (Figure 6c). In the 17 remaining SNr cells out of the 54 (31.5%), excitation without inhibition was recorded, consisting in one (3 cells, Figure 6d) or two (7 cells; Figure 6e) short latency excitations the more often followed (9 cells) by a late latency excitation. All the components were found together in 17% (n = 9) of the responding cells. Figure 6f provides the pie-chart of the different types of responses expressed as percent of total responding cells. The characteristics of each of these components were determined by pooling all evoked responses together to measure the latency (L) and the duration (D) of each events as well as the amplitude (A) of the excitations. Results are summarized in Table 2.

There was no obvious topographical distribution of the SNr cells presenting those different complex responses to Pf stimulation and these responses were reproducible overtime in a given neuron for identical stimulation parameters. By contrast, modifying the

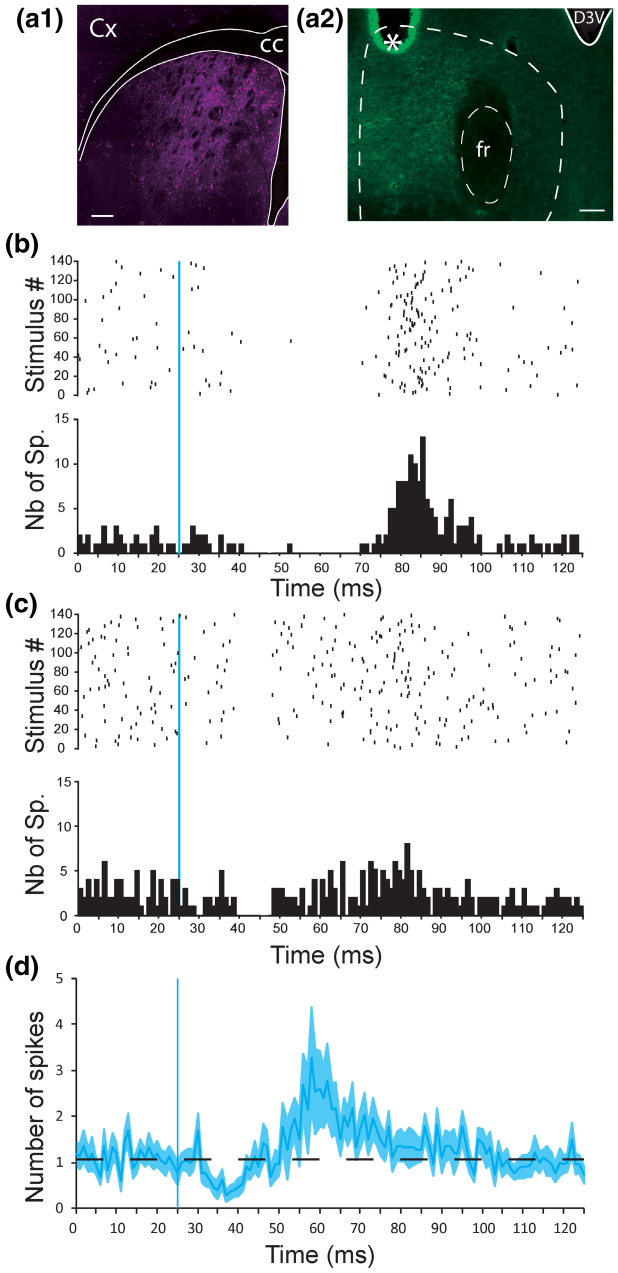

(e)

N = 18	Inhibition (18)	Late Excitation (14)
Latency (ms)	9.3 ± 1.9	30.5 ± 3.9
Duration (ms)	17.4 ± 1.7	16.8 ± 2.0
Amplitude (Nb Spikes)		34.4 ± 9.1

FIGURE 3 Responses evoked in the SNr by the photoactivation of Pf neurons projecting to the striatum. (a) representative images illustrating the virus injection site in the striatum, as shown by mCherry immunodetection (a1), and the resulting retrograde transduction of ChR2 in the Pf as visualized by YFP immunodetection (a2); the asterisk marks the tip of the optical fiber. (b,c) raster plots and PSTH (1 ms bins) illustrating examples of evoked responses that consisted in either an inhibition followed by an excitation (b) or a single inhibition (c). (d) population PSTH of the overall responses evoked in SNr neurons ($n = 18$ cells from $N = 5$ animals, 2 males and 3 females). PSTHs, generated from 140 stimulation trials, are aligned on the light pulse delivery (vertical blue line) and the light shaded color represents *SEM*. (e) characteristics of the responses evoked. cc, corpus callosum; cx, cerebral cortex; D3V, dorsal third ventricle; fr, fasciculus retroflexus; Nb of Sp., number of spikes. Scale bars: 200 μm in a1 and 100 μm in a2

intensity or the current polarity of the stimulation could alter the respective weight of each component of the evoked responses, or evoke different patterns of responses in the same individual neuron (not shown), presumably by recruiting populations of Pf neurons with different projections within the BG network.

The complex responses evoked by Pf electrical stimulation in SNr neurons were reminiscent of the responses evoked by cortical stimulation (Maurice et al., 1999). Whether electrical stimulation of the Pf recruits the cerebral cortex and remotely activates the corticostriatal pathway either orthodromically via thalamocortical projections, or through axonal reflex via cortical axons branching both in the thalamus and the striatum is an important matter of concern. The possibility of orthodromic recruitment is limited by the sparse innervation of the cerebral cortex from the Pf. The above reported lack of EYFP expression in VGluT1-labeled terminals within the Pf after virus injection in the striatum suggest that collaterals of corticostriatal projections are weak, if present, in mice; as previously reported in cat (Paré & Smith, 1996; Royce, 1983). To nevertheless exclude contribution of axonal reflex, we developed an optogenetic strategy to achieve selective activation the Pf neurons and compared the elicited responses with those evoked by electrical Pf stimulation. This was done by expressing ChR2-mCherry specifically in Pf neurons by injecting Cre-dependent AAV5 carrying the ChR2-mCherry into the Pf of mice expressing Cre under the promoter of the CaMKII, a marker of projection neurons including those of the thalamus and the cerebral cortex. 5 weeks following AAV injections into the Pf, numerous mCherry-expressing neurons were found in the Pf (Figure 7a), whereas no mCherry neuron was detected into the cerebral cortex (Figure 7b), confirming that corticothalamic neurons in our experimental setting do not express ChR2. Moreover, contrasting with the dense network of fibers in the striatum, very sparse mCherry fibers were detected in the cerebral cortex (Figure 7c), in compliance with the literature. Together, these data support the view that the responses driven by light delivery locally into the Pf will result most directly from the activation of Pf neurons.

Responses evoked by photostimulation of Pf neurons were then investigated in 41 SNr responding cells recorded in 5 CaMKII$^{cre/+}$ mice (Figure 8), 8–10 weeks post-AAV injection into the Pf. Similar to the electrical stimulation, in most tested cells ($n = 37$ of 41 responding neurons; 90%), photostimulation of the Pf induced an inhibition (Figure 8a–c), that was, in 27 out of 37 of the cells, preceded and/or followed by excitation. In the 4 (10%) remaining cells, Pf stimulation evoked only excitation (Figure 8d,e). Figure 8f summarizes the different patterns of responses expressed as percent of total responding cells. Note that the variety and the distribution of the

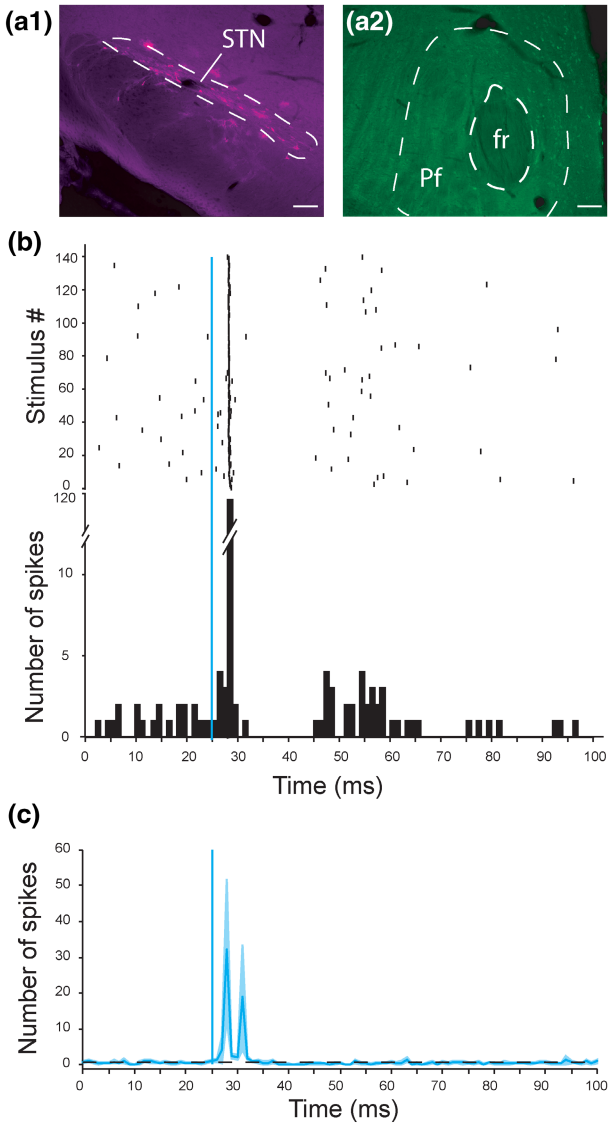

(d)

N = 8	Excit. 1 (6)	Excit. 2 (4)	Inhibition (5)
Latency (ms)	2.7 ± 0.4	6.0 ± 0.4	9.6 ± 2.3
Duration (ms)	3.5 ± 0.9	3.0 ± 1.3	25.2 ± 4.8
Amplitude (Nb Spikes)	53.9 ± 26.9	37.6 ± 29.0	

FIGURE 4 Responses evoked in the SNr by the photoactivation of Pf neurons projecting to the STN. (a) Representative images illustrating the virus injection site in the STN, as shown by mCherry immunodetection (a1), and the resulting retrograde transduction of ChR2 in the Pf as visualized by YFP immunodetection (a2). (b) raster plot and PSTH (1 ms bins) of an evoked response consisting in an excitation followed by an inhibition. (c) population PSTH of the responses evoked in SNr neurons ($n = 8$ cells from $N = 4$ animals, 1 male and 3 females) expressed as in Figure 3. (d) characteristics of the responses evoked. Excit., excitation; fr, fasciculus retroflexus; STN, subthalamic nucleus. Scale bars: 100 μm in a1 and a2

components were similar to those recorded under electrical stimulation (Figure 8f). As for the electrical stimulation, no obvious topographical distribution of the cells with distinct types of responses could be observed. Here again, the characteristics of each component were determined by pooling these complex responses altogether to calculate the latency and the duration of each component as well as the amplitude for the excitations. Table 2 summarizes the characteristics of each component of the responses evoked by electrical and optogenetic activation of Pf. Differences between the two modes of stimulation were not obvious.

3.3 | Dual retrograde labeling of Pf neurons from the STN and the SNr

To investigate whether Pf neurons projecting to the STN and to the SNr were branched, two fluorophore-conjugated variants of CTB were injected into the STN and the SNr in 3 mice. The labeling at the injection sites covered the anterior 2/3 and the lateral 2/3 extents of both structures. 231 Pf cells were retrogradely labeled with Alexa Fluor 488-CTB injected into the STN and 165 cells with Alexa Fluor 594-CTB injected into the SNr. A large population of cells showed co-localization of the two markers (Figure 9), representing 40.9 ± 12.1% of the cells labeled in the Pf from both targets. The observation of these double-labeled neurons indicates that thalamosubthalamic and thalamonigral pathways arise in significant proportion from branched Pf neurons projecting to both sites. Using a similar approach, and in agreement with the literature (Féger et al., 1994; Watson et al., 2021), we confirmed that, on the contrary, Pf-STR and Pf-STN projections arise from largely segregated populations, as shown by the fact that only 3.0 ± 2.0% of the cells showed co-labeling among 342 Pf cells retrogradely labeled from the STR and 246 labeled from the STN.

4 | DISCUSSION

This study provides physiological evidence for functional connections between the Pf and the main input (striatum and STN) and output (SNr) structures of the BG, and for possible convergence of the information conveyed though these pathways on single SNr neuron. They further indicate that the information processed through transstriatal and extrastriatal projections arises from functionally segregated populations of Pf neurons, whereas information conveyed through the STN and direct nigral projections originates from partly overlapping populations, as confirmed by retrograde tracing.

While highly reproducible in a given cell for a given setting of stimulation parameter, the responses were variable from cell to cell, as reported previously regarding the transfer of cortical information through the BG (Maurice et al., 1999). This variability is likely due to the topographical relationship between the stimulated Pf region and the recorded SNr neuron. This interpretation is consistent with the observation that modifying the stimulation intensity or polarity can impact the response pattern, presumably due to the recruitment of a less or more extended region of the Pf connected with the recorded neuron. The composition of the evoked responses is unlikely

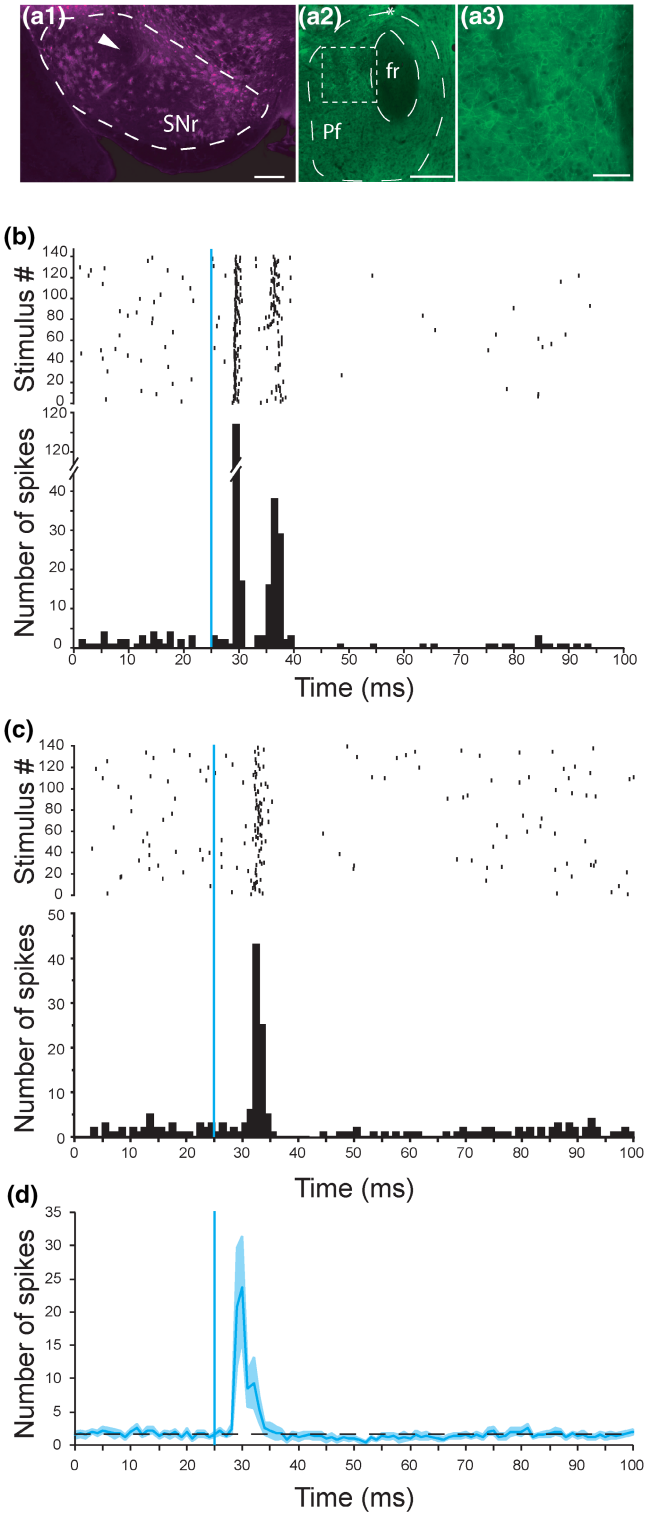

(e)

N = 14	Excit. 1 (7)	Excit. 2 (9)	Inhibition (7)
Latency (ms)	3.4 ± 0.3	6.9 ± 0.5	8.6 ± 0.6
Duration (ms)	2.8 ± 0.5	4.3 ± 0.8	18.3 ± 4.4
Amplitude (Nb Spikes)	51.4 ± 15.0	40.4 ± 8.0	

FIGURE 5 Responses evoked in SNr by the photoactivation of Pf neurons projecting to the SNr. Representative images illustrating the virus injection site in the SNr, as shown by mCherry immunodetection (a1), and the resulting retrograde transduction of ChR2 in the Pf as visualized by YFP immunodetection (a2 and magnification in a3); arrowhead indicates the canula track and asterisk marks the tip of the optical fiber. The evoked responses consisted in early excitations (b,c) that were often followed by an inhibition. (d) Population PSTH of the responses evoked in SNr neurons ($n = 14$ cells from $N = 6$ animals, 3 males and 3 females) expressed as in Figure 3. (e) Characteristics of the responses evoked. Excit., excitation; Fr, fasciculus retroflexus; Pf, parafascicular nucleus; SNr, substantia nigra pars reticulata. Scale bars: 200 μm in a1 and a2; 50 μm in a3

to be affected by the anesthesia. For instance, one can note that cortical stimulation evokes similar triphasic responses (excitation–inhibition–excitation) in SNR neurons in awake animals and under different anesthesia (Degos et al., 2005; Koketsu et al., 2021; Maurice et al., 1999; Nishimuta et al., 2002; Sano et al., 2013). However, we cannot exclude an impact of the anesthesia on the characteristics (latency, duration, and amplitude) of the response components.

In the different stimulation paradigms tested, the responses were usually polymodal, suggesting the involvement of different subcircuits, even when targeting neurons identified based on their connectivity with a given component of the BG. This was expected for the neurons projecting to the striatum, as the information can be processed through the direct and the indirect trans-striatal pathways, but not for neurons projecting to the STN or SNr. For instance, optogenetic stimulation of the Pf neurons projecting to the striatum elicited an inhibition, the most often followed by an excitation. These responses can be attributed to the recruitment of striatal medium spiny neurons (MSNs) of the direct and of the indirect pathway, respectively, which exert inhibitory versus excitatory influence onto SNr neurons. Indeed, thalamostriatal terminals have been reported to target both types of MSNs, with the direct pathway MSNs receiving a greater density of thalamic synapses than those of the indirect pathway (Huerta-Ocampo et al., 2014), which could account for the more consistent recording of the inhibitory versus the late excitatory component of the responses. One cannot exclude a role of striatal interneurons, in particular cholinergic interneurons. These interneurons receive particularly dense Pf innervation and can exert complex influence on MSNs by acting via different subtypes of muscarinic cholinergic receptor, by co-releasing glutamate (Higley et al., 2011) and indirectly via the control of GABA release by dopaminergic terminals (Nelson et al., 2014) and interneurons via nicotinic receptors (English et al., 2012; Faust et al., 2015, 2016; Luo et al., 2013). Activation of Pf neurons projecting to either the STN or the SNr unexpectedly elicited complex responses, consisting of one or two early excitations followed in most cases by a brief inhibition. The lack of such early excitation component in the responses elicited by the activation of Pf neurons

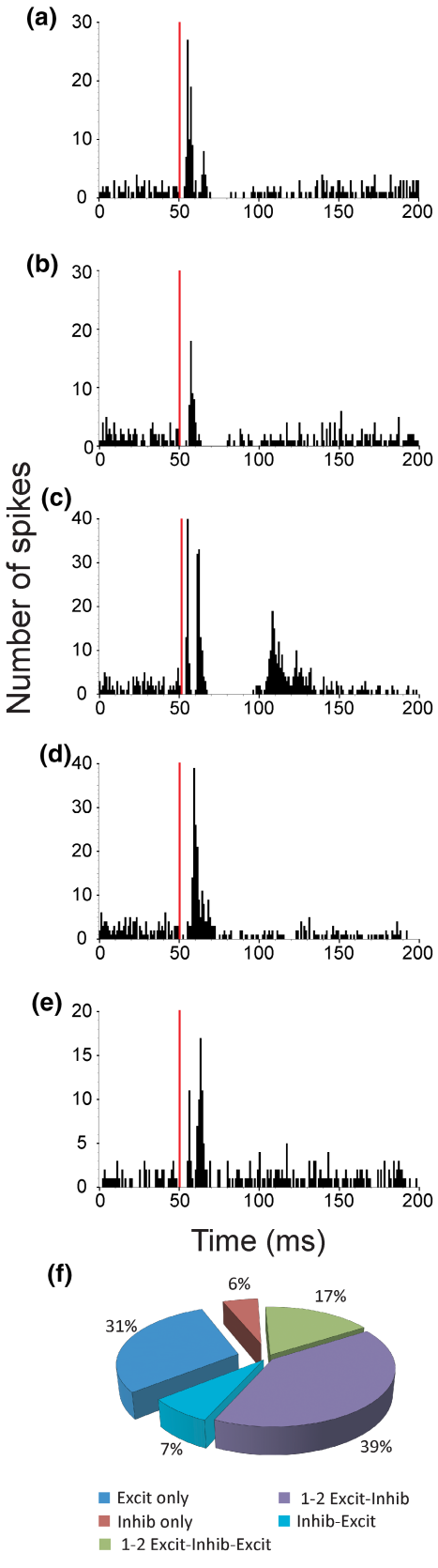

FIGURE 6 Patterns of responses evoked in SNr cells by Pf electrical stimulation. (a–e) representative PSTHs (1 ms bins) illustrating the diversity of the responses recorded in individual SNr neurons; red lines indicate the time of electrical shock delivery. (f) pie-chart illustrating the percentage of each type of responses exhibited by the overall responding cells ($n = 54$ cells from $N = 18$ animals, 10 males and 8 females). Excit, excitation; Inhib, inhibition

projecting to the striatum suggests that these neurons do not provide significant functional input to the STN or the SNr. This complies with and extends previous observations in the rat (Féger et al., 1994) and the mouse (Watson et al., 2021) showing that the Pf projections to the STN and striatum arise mostly from separate neuronal populations. Indeed, they emphasize a functional segregation of Pf information processing via the striatum and extrastriatal sites. Such a segregation supports the view of differential implication in BG functions, as recently exemplified by the demonstration of the contribution of Pf projections to STN but not to striatum in movement initiation (Watson et al., 2021). The fact that the activation of Pf neurons projecting to either the STN or the SNr triggers excitations with similar bimodal distribution, or even two excitations in the same cell, suggests that the two structures are connected (at least in part) by the same thalamic neuronal population. This is confirmed by our dual retrograde fluorescent labeling using CTB, showing that a non-negligible proportion of Pf neurons targeting these structures innervate both of them. Therefore, stimulation of Pf neurons projecting to either the STN or the SNr would trigger both a monosynaptic and a di-synaptic response. These responses will involve, respectively, collateralized and non-collateralized projections for STN and vice versa for SNr. In principle, light delivery in the Pf following viral injection in the SNr might also trigger antidromic activation of SNr neurons that reciprocally project to the Pf (Tsumori et al., 2000). However, antidromic SNr activation is unlikely to account for the early excitations because they do not show a fixed latency and do not collide with spontaneous orthodromic spikes emitted by SNr neurons. Regarding the brief inhibition that in most cases follows the early excitatory responses, it could result from the recruitment of the potent inhibitory microcircuit formed by the dense network of intranigral recurrent collaterals (Brown et al., 2014; Deniau et al., 1982). One cannot exclude, however, the contribution of the thalamic input to the globus pallidus, which could result in SNr inhibition either directly or via STN inhibition in our experimental paradigm if Pf projections to the STN and the SNr are collaterals of projections to the globus pallidus. Finally, the recently evidenced efferent projections of the STN neurons innervated by the Pf onto the globus pallidus in addition to the SNr (Watson et al., 2021) might also be involved.

After having characterized the responses elicited in the SNr by optogenetic activation of neuronal subpopulations of Pf distinguished on the basis of their connectivity with the striatum, the STN, and the SNr, we aimed at examining whether and how the information processed through these pathways are integrated in the BG output structure. To do so, we examined the responses evoked by activation of Pf neuronal populations as a whole using either electrical stimulation or optogenetics. The response patterns were highly similar in the two paradigms, excluding major contribution,

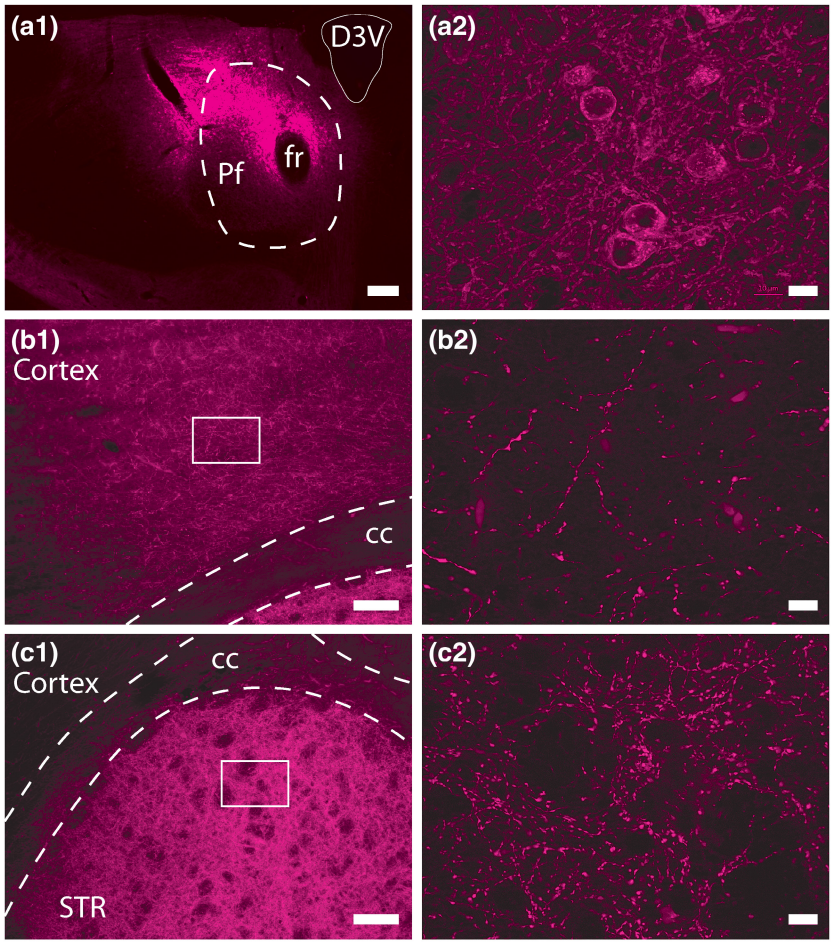

FIGURE 7 Representative photomicrographs of the typical mCherry expression patterns in coronal sections at the level of the Pf (a), the cerebral cortex (b), and the striatum (c) of a transgenic CaMKII$^{cre/+}$ mice following AAV-ChR2-mCherry virus injection into the Pf. mCherry expression is revealed by immunostaining with an antibody against RFP (magenta). The right panels (scale 10 μm) are magnification of the boxed areas in the corresponding left panels (scale 100 μm). Both labeled cell bodies and neurites were observed in the Pf (a1,a2), whereas the cerebral cortex (b1,b2) and the striatum (c1,c2) contained only axonal fibers. Note the very sparse cortical staining compared with the dense striatal labeling. cc, *corpus callosum*; D3V, dorsal third ventricle; fr, *fasciculus retroflexus*; Pf, parafascicular nucleus; STR, striatum. Scale bars: 200 μm in a1–c1 and 10 μm in a2–c2

in the responses to electrical Pf stimulation, of axonal reflex involving pathways collateralizing onto both Pf and a BG component, as the projections from the cerebral cortex that branch in the Pf and striatum (Paré & Smith, 1996). These responses were in most cases multiphasic, the more complex including four components, namely two early excitations followed by an inhibition and a late excitation. Given the connectivity-based responses reported above, the early excitations are likely to result from the recruitment of the trans-subthalamic and direct nigral pathways, the inhibition from recruitment of the trans-striatal direct pathway (presumably reinforced by local inhibitory microcircuits following SNr activation or recruitment of globus pallidus), and the late excitation from the activation of the indirect trans-striatal pathway. Taken as a whole, these data suggest that, although Pf projections to extrastriatal structures are weak in terms of density of innervation, as compared to the massive thalamostriatal pathway, they should not be considered as functionally less important, since they have the potential to shape the activity of SNr neurons. Previous work in monkey called for a reappraisal of the functional weight of extrastriatal Pf projections based on the observation that their long arborization, although poorly branched, covered a relatively large portion of each BG nucleus (Tandé et al., 2006). Moreover, in the rat, axons from the Pf have been shown to contact more proximal dendrites of STN neurons (Bevan et al., 1995), which places them in position to exert potent action onto the contacted neurons. If this is a general feature of extrastriatal projections, thalamic axons could then exert powerful action on the different components of the BG network.

In conclusion, our study shows that the trans-striatal, trans-subthalamic, and direct nigral pathways formed from Pf neurons are functional and although more or less segregated can provide converging information onto SNr neurons. The responses Pf activation as a whole in the SNr thus provide a read-out of the functionality of the different subcircuits by which information from

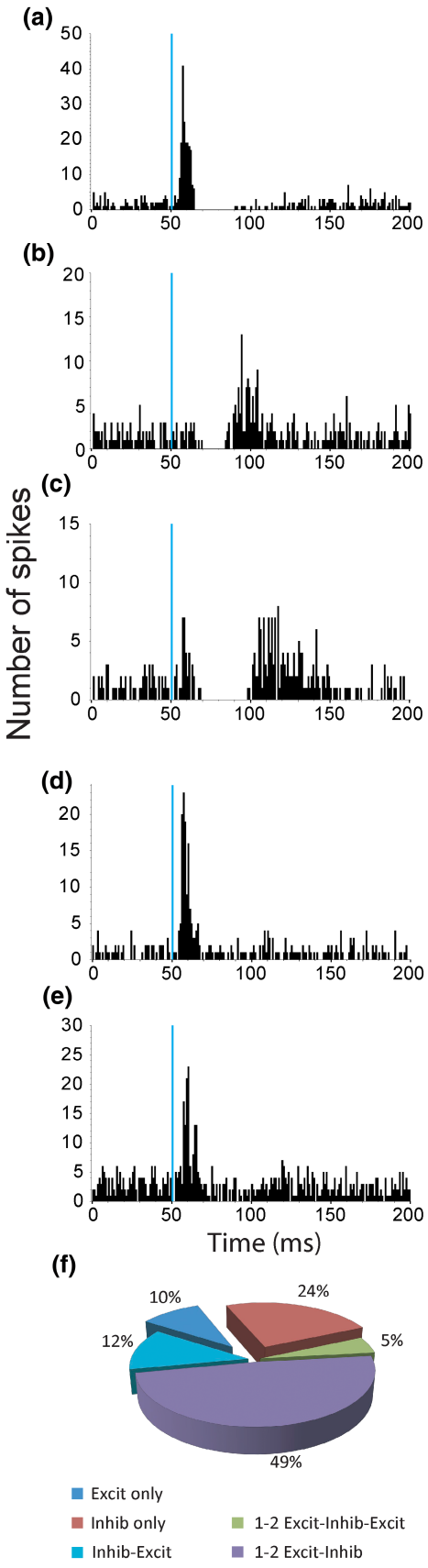

FIGURE 8 Patterns of responses evoked in SNr cells by Pf photostimulation. (a–e) representative PSTHs (1 ms bins) illustrating the diversity of the responses evoked in distinct SNr cells and their similarity with those induced by Pf electrical stimulation (see Figure 6); blue lines indicate the time of light flash (1 ms) delivery. (f) pie-chart of the percentage of each type of response in the overall responding cells ($n = 41$ cells from $N = 4$ animals, 1 male and 3 females). Excit, excitation; Inhib, inhibition

the Pf can be processed through the BG to regulate the network outflow, which might be useful to detect changes in these circuits occurring in different treatment or pathological conditions, as previously done for the cortically driven BG circuits. Here, Pf neuronal populations were activated artificially either together or separately based on their connectivity, and what remains to be determined is whether and when these different components of the thalamo-BG circuits are recruited under physiological conditions in connection with behavior. Recent evidence has been provided for converging thalamic and cortical information onto direct and indirect MSNs in the striatal matrix, with a predominance of the cortical input (Huerta-Ocampo et al., 2014). Moreover, distinct cortical–thalamic–striatal circuits through the Pf have been revealed, placing this thalamic complex as a critical node that organizes limbic, associative, and somatosensory information in the BG (Mandelbaum et al., 2019). Whether cortical and thalamic projections to STN neurons are also organized in such sophisticated circuits would need to be investigated. In addition, Pf is in position to also provide direct information to the output structures of the network. Characterizing the information that flows within the BG through striatal and extrastriatal thalamic pathways is then a major issue that needs to be addressed to fully appreciate Pf implication in BG functioning in physiological and pathological conditions.

DECLARATION OF TRANSPARENCY

The authors, reviewers and editors affirm that in accordance to the policies set by the *Journal of Neuroscience Research*, this manuscript presents an accurate and transparent account of the study being reported and that all critical details describing the methods and results are present.

ACKNOWLEDGMENTS

This work was granted by Fondation de France (2013-00043175 and 2014-00053111) and supported by CNRS and Aix-Marseille University. It was conducted within the context of the DHUNE project supported by A*MIDEX (ANR-11-IDEX-0001-02). IBDM is affiliated with the Institute NeuroMarseille and the graduate School NeuroSchool supported by the French government under the Programme "Investissements d'Avenir", Initiative d'Excellence d'Aix-Marseille Université via A*Midex funding (AMX-19-IET-004) and ANR (ANR-17-EURE-0029). Microscopy was performed at the imaging platform of the IBDM, supported by the ANR through the "Investments for the Future" program (France-BioImaging, ANR-10-INSB-04-01). MHD was awarded a PhD excellence fellowship from the Ministry of Higher Education and Research of Tunisia. We thank Jean-Pierre Kessler for helpful discussion and help with the confocal microscopy.

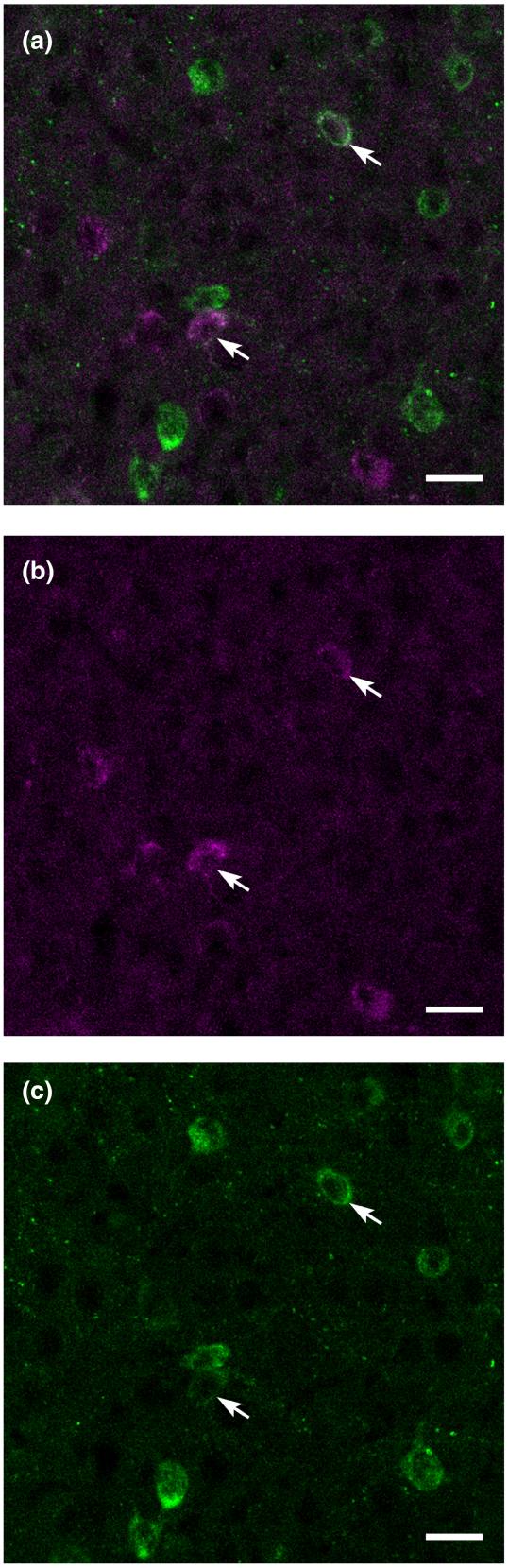

FIGURE 9 Confocal image of retrogradely labeled cell bodies in the Pf after Alexa Fluor 488-CTB injection into the STN (green) combined with Alexa Fluor 594-CTB injection into the SNr (magenta). (a) merged image; (b,c) single channels. The dually labeled cells are indicated by arrows. Scale bar: 20 μm

CONFLICT OF INTEREST

The authors declare no competing financial interests.

AUTHOR CONTRIBUTIONS

All authors had full access to all the data in the study and take responsibility for the integrity of the data and the accuracy of the data analysis. *Conceptualization*, N.M. and L.K.-L.G.; *Investigation*, M.H.-D., F.J., P.S., and N.M.; *Formal analysis*, M.H.-D. and N.M.; *Writing – Original Draft*, N.M. and L.K.-L.G.; *Writing—Review & Editing*, N.M. and L.K.-L.G.; *Funding Acquisition*, N.M. and L.K.-L.G.

PEER REVIEW

The peer review history for this article is available at https://publons.com/publon/10.1002/jnr.25046.

DATA AVAILABILITY STATEMENT

Data available on request from the authors.

ORCID

Pascal Salin https://orcid.org/0000-0003-1733-2856
Lydia Kerkerian-Le Goff https://orcid.org/0000-0002-7951-3479
Nicolas Maurice https://orcid.org/0000-0001-5638-5403

REFERENCES

Abudukeyoumu, N., Hernandez-Flores, T., Garcia-Munoz, M., & Arbuthnott, G. W. (2019). Cholinergic modulation of striatal microcircuits. *European Journal of Neuroscience*, *49*, 604–622.

Bevan, M. D., Francis, C. M., & Bolam, J. P. (1995). The glutamate-enriched cortical and thalamic input to neurons in the subthalamic nucleus of the rat: Convergence with GABA-positive terminals. *Journal of Comparative Neurology*, *361*, 491–511.

Brown, H. D., Baker, P. M., & Ragozzino, M. E. (2010). The parafascicular thalamic nucleus concomitantly influences behavioral flexibility and dorsomedial striatal acetylcholine output in rats. *Journal of Neuroscience*, *30*, 14390–14398.

Brown, J., Pan, W. X., & Dudman, J. T. (2014). The inhibitory microcircuit of the substantia nigra provides feedback gain control of the basal ganglia output. *eLife*, *2014*, 1–25.

Bunney, B. S., Walters, J. R., Roth, R. H., & Aghajanian, G. K. (1973). Dopaminergic neurons: Effect of antipsychotic drugs and amphetamine on single cell activity. *Journal of Pharmacology and Experimental Therapeutics*, *185*, 560–571.

Castle, M., Aymerich, M. S., Sanchez-Escobar, C., Gonzalo, N., Obeso, J. A., & Lanciego, J. L. (2005). Thalamic innervation of the direct and indirect basal ganglia pathways in the rat: Ipsi- and contralateral projections. *Journal of Comparative Neurology*, *483*, 143–153.

Degos, B., Deniau, J. M., Thierry, A. M., Glowinski, J., Pezard, L., & Maurice, N. (2005). Neuroleptic-induced catalepsy: Electrophysiological mechanisms of functional recovery induced by high-frequency stimulation of the subthalamic nucleus. *Journal of Neuroscience*, *25*, 7687–7696.

Deniau, J. M., Hammond, C., Riszk, A., & Féger, J. (1978). Electrophysiological properties of identified output neurons of the rat substantia nigra (pars compacta and pars reticulata): Evidences for the existence of branched neurons. *Experimental Brain Research*, *32*, 409–422.

Deniau, J. M., Kitai, S. T., Donoghue, J. P., & Grofova, I. (1982). Neuronal interactions in the substantia nigra pars reticulata through axon

collaterals of the projection neurons. An electrophysiological and morphological study. *Experimental Brain Research*, *47*, 105–113.

Deschênes, M., Bourassa, J., Doan, V. D., & Parent, A. (1996). A single-cell study of the axonal projections arising from the posterior Intralaminar thalamic nuclei in the rat. *European Journal of Neuroscience*, *8*, 329–343.

Ding, J. B., Guzman, J. N., Peterson, J. D., Goldberg, J. A., & Surmeier, D. J. (2010). Thalamic gating of corticostriatal signaling by cholinergic interneurons. *Neuron*, *67*, 294–307.

English, D. F., Ibanez-Sandoval, O., Stark, E., Tecuapetla, F., Buzsáki, G., Deisseroth, K., Tepper, J. M., & Koos, T. (2012). GABAergic circuits mediate the reinforcement-related signals of striatal cholinergic interneurons. *Nature Neuroscience*, *15*, 123–130.

Fasano, A., Daniele, A., & Albanese, A. (2012). Treatment of motor and non-motor features of Parkinson's disease with deep brain stimulation. *Lancet Neurology*, *11*, 429–442.

Faust, T. W., Assous, M., Shah, F., Tepper, J. M., & Koós, T. (2015). Novel fast adapting interneurons mediate cholinergic-induced fast $GABA_A$ inhibitory postsynaptic currents in striatal spiny neurons. *European Journal of Neuroscience*, *42*, 1764–1774.

Faust, T. W., Assous, M., Tepper, J. M., & Koós, T. (2016). Neostriatal GABAergic interneurons mediate cholinergic inhibition of spiny projection neurons. *Journal of Neuroscience*, *36*, 9505–9511.

Féger, J., Bevan, M., & Crossman, A. R. (1994). The projections from the parafascicular thalamic nucleus to the subthalamic nucleus and the striatum arise from separate neuronal populations: A comparison with the corticostriatal and corticosubthalamic efferents in a retrograde fluorescent double-labell. *Neuroscience*, *60*, 125–132.

Gradinaru, V., Zhang, F., Ramakrishnan, C., Mattis, J., Prakash, R., Diester, I., Goshen, I., Thompson, K. R., & Deisseroth, K. (2010). Molecular and cellular approaches for diversifying and extending optogenetics. *Cell*, *141*, 154–165.

Henderson, J. M., Carpenter, K., Cartwright, H., & Halliday, G. M. (2000). Degeneration of the centre median-parafascicular complex in Parkinson's disease. *Annals of Neurology*, *47*, 345–352.

Higley, M. J., Gittis, A. H., Oldenburg, I. A., Balthasar, N., Seal, R. P., Edwards, R. H., Lowell, B. B., Kreitzer, A. C., & Sabatini, B. L. (2011). Cholinergic interneurons mediate fast VGluT3-dependent glutamatergic transmission in the striatum. *PLoS ONE*, *6*, e19155.

Huerta-Ocampo, I., Mena-Segovia, J., & Bolam, J. P. (2014). Convergence of cortical and thalamic input to direct and indirect pathway medium spiny neurons in the striatum. *Brain Structure & Function*, *219*, 1787–1800.

Ilyas, A., Pizarro, D., Romeo, A. K., Riley, K. O., & Pati, S. (2019). The centromedian nucleus: Anatomy, physiology, and clinical implications. *Journal of Clinical Neuroscience*, *63*, 1–7.

Kerkerian-Le Goff, L., Jouve, L., Melon, C., & Salin, P. (2009). Rationale for targeting the thalamic centre-median parafascicular complex in the surgical treatment of Parkinson's disease. *Parkinsonism & Related Disorders*, *15*, S167–S170.

Koketsu, D., Chiken, S., Hisatsune, T., Miyachi, S., & Nambu, A. (2021). Elimination of the cortico-subthalamic hyperdirect pathway induces motor hyperactivity in mice. *Journal of Neuroscience*, *41*, 5502–5510.

Lanciego, J. L., Gonzalo, N., Castle, M., Sanchez-Escobar, C., Aymerich, M. S., & Obeso, J. A. (2004). Thalamic innervation of striatal and subthalamic neurons projecting to the rat entopeduncular nucleus. *European Journal of Neuroscience*, *19*, 1267–1277.

Lanciego, J. L., López, I. P., Rico, A. J., Aymerich, M. S., Pérez-Manso, M., Conte, L., Combarro, C., Roda, E., Molina, C., Gonzalo, N., Castle, M., Tuñón, T., Erro, E., & Barroso-Chinea, P. (2009). The search for a role of the caudal intralaminar nuclei in the pathophysiology of Parkinson's disease. *Brain Research Bulletin*, *78*, 55–59.

Lapper, S. R., & Bolam, J. P. (1992). Input from the frontal cortex and the parafascicular nucleus to cholinergic interneurons in the dorsal striatum of the rat. *Neuroscience*, *51*, 533–545.

Luo, R., Janssen, M. J., Partridge, J. G., & Vicini, S. (2013). Direct and GABA-mediated indirect effects of nicotinic ACh receptor agonists on striatal neurones. *Journal of Physiology*, *591*, 203–217.

Mandelbaum, G., Taranda, J., Haynes, T. M., Hochbaum, D. R., Huang, K. W., Hyun, M., Umadevi Venkataraju, K., Straub, C., Wang, W., Robertson, K., Osten, P., & Sabatini, B. L. (2019). Distinct cortical-thalamic-striatal circuits through the parafascicular nucleus. *Neuron*, *102*, 636–652.e7.

Marini, G., Pianca, L., & Tredici, G. (1999). Descending projections arising from the parafascicular nucleus in rats: Trajectory of fibers, projection pattern and mapping of terminations. *Somatosensory & Motor Research*, *16*, 207–222.

Matsumoto, N., Minamimoto, T., Graybiel, A. M., & Kimura, M. (2001). Neurons in the thalamic CM-pf complex supply striatal neurons with information about behaviorally significant sensory events. *Journal of Neurophysiology*, *85*, 960–976.

Maurice, N., Deniau, J. M., Glowinski, J., & Thierry, A. M. (1999). Relationships between the prefrontal cortex and the basal ganglia in the rat: Physiology of the cortico-nigral circuits. *Journal of Neuroscience*, *19*, 4674–4681.

Nelson, A. B., Hammack, N., Yang, C. F., Shah, N. M., Seal, R. P., & Kreitzer, A. C. (2014). Striatal cholinergic interneurons drive GABA release from dopamine terminals. *Neuron*, *82*, 63–70.

Nishimuta, K., Sasamoto, K., & Ninomiya, Y. (2002). Neural activities in the substantia nigra modulated by stimulation of the orofacial motor cortex and rhythmical jaw movements in the rat. *Neuroscience*, *113*, 915–923.

Paré, D., & Smith, Y. (1996). Thalamic collaterals of corticostriatal axons: Their termination field and synaptic targets in cats. *Journal of Comparative Neurology*, *372*, 551–567.

Paxinos, G., & Franklin, K. B. J. (2001). *The mouse brain in stereotaxic coordinates* (Harcourt, ed). (2nd ed.). Academic Press.

Pinault, D. (1996). A novel single-cell staining procedure performed in vivo under electrophysiological control: Morpho-functional features of juxtacellularly labeled thalamic cells and other central neurons with biocytin or neurobiotin. *Journal of Neuroscience Methods*, *65*, 113–136.

Royce, G. J. (1983). Cortical neurons with collateral projections to both the caudate nucleus and the centromedian-parafascicular thalamic complex: A fluorescent retrograde double labeling study in the cat. *Experimental Brain Research*, *50*, 157–165.

Sadikot, A. F., Parent, A., & François, C. (1992). Efferent connections of the centromedian and parafascicular nuclei in the squirrel monkey: A PHA-L study of the subcortical projections. *Journal of Comparative Neurology*, *315*, 137–159.

Sadikot, A. F., & Rymar, V. V. (2009). The primate centromedian-parafascicular complex: Anatomical organization with a note on neuromodulation. *Brain Research Bulletin*, *78*, 122–130.

Sano, H., Chiken, S., Hikida, T., Kobayashi, K., & Nambu, A. (2013). Signals through the striatopallidal indirect pathway stop movements by phasic excitation in the substantia nigra. *Journal of Neuroscience*, *33*, 7583–7594.

Sidibé, M., & Smith, Y. (1999). Thalamic inputs to striatal interneurons in monkeys: Synaptic organization and co-localization of calcium binding proteins. *Neuroscience*, *89*, 1189–1208.

Smith, Y., Raju, D., Nanda, B., Pare, J.-F., Galvan, A., & Wichmann, T. (2009). The thalamostriatal systems: Anatomical and functional organization in normal and parkinsonian states. *Brain Research Bulletin*, *78*, 60–68.

Smith, Y., Raju, D. V., Pare, J.-F., & Sidibe, M. (2004). The thalamostriatal system: A highly specific network of the basal ganglia circuitry. *Trends in Neurosciences*, *27*, 520–527.

Stefani, A., Peppe, A., Pierantozzi, M., Galati, S., Moschella, V., Stanzione, P., & Mazzone, P. (2009). Multi-target strategy for parkinsonian patients: The role of deep brain stimulation in the centromedian-parafascicularis complex. *Brain Research Bulletin*, *78*, 113–118.

Tandé, D., Féger, J., Hirsch, E. C., & François, C. (2006). Parafascicular nucleus projection to the extrastriatal basal ganglia in monkeys. *Neuroreport*, *17*, 277–280.

Testini, P., Min, H.-K., Bashir, A., & Lee, K. H. (2016). Deep brain stimulation for Tourette's syndrome: The case for targeting the thalamic centromedian-parafascicular complex. *Frontiers in Neurology*, *7*, 193.

Tsumori, T., Yokota, S., Lai, H., & Yasui, Y. (2000). Monosynaptic and disynaptic projections from the substantia nigra pars reticulata to the parafascicular thalamic nucleus in the rat. *Brain Research*, *858*, 429–435.

Watson, G. D. R., Hughes, R. N., Petter, E. A., Fallon, I. P., Kim, N., Severino, F. P. U., & Yin, H. H. (2021). Thalamic projections to the subthalamic nucleus contribute to movement initiation and rescue of parkinsonian symptoms. *Science Advances*, *7*, 1–13.

Yamanaka, K., Hori, Y., Minamimoto, T., Yamada, H., Matsumoto, N., Enomoto, K., Aosaki, T., Graybiel, A. M., & Kimura, M. (2018). Roles of centromedian parafascicular nuclei of thalamus and cholinergic interneurons in the dorsal striatum in associative learning of environmental events. *Journal of Neural Transmission*, *125*, 501–513.

Yasukawa, T., Kita, T., Xue, Y., & Kita, H. (2004). Rat intralaminar thalamic nuclei projections to the globus pallidus: A biotinylated dextran amine anterograde tracing study. *Journal of Comparative Neurology*, *471*, 153–167.

SUPPORTING INFORMATION

Additional supporting information may be found in the online version of the article at the publisher's website.

Transparent Science Questionnaire for Authors

How to cite this article: Hanini-Daoud, M., Jaouen, F., Salin, P., Kerkerian-Le Goff, L. & Maurice, N. (2022). Processing of information from the parafascicular nucleus of the thalamus through the basal ganglia. *Journal of Neuroscience Research*, 100, 1370–1385. https://doi.org/10.1002/jnr.25046